Time-resolved measurements of nanoscale surface pattern formation kinetics in two dimensions on ion-irradiated Si

Eitan Anzenberg,[1,*] Charbel S. Madi,[2] Michael J. Aziz,[2] and Karl F. Ludwig Jr.[1]
[1]*Department of Physics, Boston University, Boston, Massachusetts 02215, USA*
[2]*Harvard School of Engineering and Applied Sciences, Cambridge, Massachusetts 02138, USA*
(Received 27 July 2011; revised manuscript received 22 November 2011; published 19 December 2011)

The nanoscale kinetics of surface topography evolution on silicon surfaces irradiated with 1 keV Ar^+ ions is examined in both directions perpendicular and parallel to the projection of the ion beam on the surface. We use grazing incidence small angle x-ray scattering to measure *in situ* the evolution of surface morphology via the linear dispersion relation. We study the transition from surface ultra-smoothening at low angles of deviation from normal ion incidence to a pattern-forming instability at high incidence angles. A model based on the effects of impact-induced redistribution of those atoms that are *not* sputtered away explains both the observed ultra-smoothening at low angles from normal ion incidence and the instability at higher angles and accounts quantitatively for the measured two-dimensional dispersion relation and its dependence on incidence angle.

DOI: 10.1103/PhysRevB.84.214108 PACS number(s): 81.16.Rf, 81.07.−b, 62.23.St

I. INTRODUCTION

Uniform ion irradiation of solid surfaces can cause ultra-smoothening[1,2] or self-organized nanoscale surface topographic pattern formation, depending on control parameters such as ion and target species, ion energy and incidence angle, target temperature, and surface impurity coverage.[2–5] Pattern periodicities as small as 7 nm[6] have caused interest in the potential of this process for sublithographic nanofabrication. The pattern-forming instability has been attributed to the surface curvature-dependence of the sputter erosion rate, as described by the model of Bradley and Harper (BH)[7] who performed a linear stability analysis of Sigmund's instability mechanism from a Gaussian ellipsoid model for the nuclear collision cascade energy density.[8] The BH model, which combines the destabilizing effect of the curvature-dependent sputter erosion rate with the stabilizing effect of surface diffusion-mediated surface smoothening, predicts that a flat surface is unstable to topographic perturbations of some wave vector under all conditions. However, although the model assumes an amorphous, monatomic target, a number of studies of noble gas ion irradiation of silicon near room temperature, which develops an amorphous surface layer and therefore represents the ideal test case, have reported that at low-ion incidence angles θ with respect to the surface normal there is instead surface ultra-smoothening and not until the angle of incidence reaches several tens of degrees is there a transition to correlated ripple structures of "parallel mode": wave vector parallel to the projection of the ion beam on the surface (x direction).[2,5,9] Some observations indicate that at sufficiently grazing incidence, the most unstable wave vector switches to "perpendicular mode" (along the y-axis, perpendicular to the ion beam). Several groups have invoked the stabilizing effect of ion impact-induced lateral mass redistribution[4,9–11] as a mechanism to offset the BH mechanism at low angles. Recently, we have presented a study of surface evolution on monatomic amorphous silicon in the x-direction that shows that both the smoothening at low angles and the transition to ripple formation at higher angles is driven predominantly by lateral mass redistribution, with the effect of sputter erosion playing an insignificant role.[12] Here we present experimental results showing that morphology evolution in both directions within the surface is consistent with a model that includes impact-induced mass redistribution and surface-confined ion-stimulated viscous flow.[13] The latter effect is always stabilizing; the former effect switches from stabilizing to destabilizing with increasing θ along the x-direction and remains stabilizing at all θ along the y-direction.

II. METHODS

A linear-stability analysis of a flat, isotropic, and monatomic surface undergoing ion bombardment while simultaneously relaxing by surface-confined viscous flow yields the following behavior for the early-time evolution of the surface topography:

$$\frac{\partial h(\mathbf{q},t)}{\partial t} = -\left[S_X(\theta)q_x^2 + S_Y(\theta)q_y^2 + B\left(q_x^2+q_y^2\right)^2\right] \times h(\mathbf{q},t) + \xi(\mathbf{q},t), \quad (1)$$

where

$$h(\mathbf{q},t) = \iint h(x,y,t)\exp(-i(q_x x + q_y y))dxdy \quad (2)$$

is the spectrum of spatial frequencies $\mathbf{q}$ in the surface topography at time t, $S_{X,Y}(\theta)$ are the θ-dependent kinetic curvature coefficients causing surface instability (stability) when negative (positive), $\xi(\mathbf{q},t)$ is a stochastic noise term reflecting the random nature of the ion-irradiation process, $B = \frac{\gamma d^3}{3\eta}$ is the parameter describing surface-confined viscous flow in the $qd \ll 1$ limit[14] where γ is the surface-free energy, η is the viscosity of the ion-stimulated layer during irradiation, and d is the thickness of the viscous layer. Integrating Eq. (1) yields the time-dependent behavior of the height-height structure factor,[15] $|h(\mathbf{q},t)|^2$:

$$|h(\mathbf{q},t)|^2 = \left(|h(\mathbf{q},0)|^2 + \frac{\alpha}{2R(\mathbf{q})}\right)\exp(2R(\mathbf{q})t) - \frac{\alpha}{2R(\mathbf{q})}, \quad (3)$$

where $h(\mathbf{q}, 0)$ is the initial roughness spectrum, α is the structure factor of the stochastic white noise, and $R(\mathbf{q})$ is the linear-dispersion relation, given by

$$R(\mathbf{q}) = -S_X q_x^2 - S_Y q_y^2 - B\left(q_x^2 + q_y^2\right)^2. \quad (4)$$

Positive $R(\mathbf{q})$ drives exponential amplification of modes of wave vector $\mathbf{q}$, leading to topographical instability, whereas negative $R(\mathbf{q})$ damps fluctuations and stabilizes modes of wave vector $\mathbf{q}$.

In this study we use grazing incidence small angle x-ray scattering (GISAXS) to characterize the surface height-height correlations *in situ* during ion bombardment. In the Born approximation the GISAXS scattering pattern is proportional to the height-height structure factor in the limit that $q_z h \ll 1$,[16] a limit that is satisfied in all our experimental conditions. Our experimental setup consists of a custom-built ultrahigh vacuum chamber with a base pressure of 1×10^{-8} Torr. Argon gas of purity 99.999% was used, and Ar ions were generated using a Physical Electronics, Inc., PHI ion gun set at 1 keV ion energy. The beam diameter was approximately 1.5 cm, and the flux during these experiments was approximately 2×10^{12} ions/(cm^{2}s) reckoned in a plane perpendicular to the ion beam. Si(001) (p type, 1–10 Ω cm) at room temperature was held clipless using silver paste on its back in the chamber with extra care taken to minimize secondary collisions that might lead to the sputtering of impurities onto the surface. X-ray photons were provided by the National Synchrotron Light Source at beamline X21. A photon wavelength of 0.124 nm was selected by a Si(111) monochromator with a flux of approximately 10^{12} photons/s. The x-ray incidence angle on the sample surface was 0.82° from grazing and a 384-pixel linear detector measured the scattering pattern with an exit angle set to the critical angle for silicon, 0.18° from grazing.

III. RESULTS

Figures 1(a) and 1(c) show the time evolution of the scattered intensity during ion bombardment for normal incidence and 80° from normal, respectively, as functions of q_y. The time evolution of each mode q_y is least-squares fit to an exponential function given by Eq. (3). Examples of evolution at typical wave numbers and fits are shown in Figs. 1(b) and 1(d). Error bars correspond to assumed Poisson counting statistics. Figure 2 shows the experimental dispersion relation $R(q_y)$ obtained from such fits for ion-incidence angles $\theta =$ 0°, 25°, 45°, 55°, 70°, and 80° from normal. For $\theta < 80°$, $R(q_y)$ is negative for all modes, and the surface is stable to perpendicular-mode ripples under bombardment. At 80°, the amplification factor at low q_y is very small in magnitude, and the sign of $R(q_y)$ is uncertain. Solid lines in Fig. 2 correspond to error bar weighted least-square fitting of the experimental $R(q_y)$ to Eq. (4), letting S_y vary at each incidence angle and letting the coefficient of the quadratic term B vary as an angle-independent coefficient. When combined with results from our previous study,[12] the best-fit experimental value is $B =$ 0.015 nm^4/s.

The data points in Fig. 3 represent the curvature coefficients controlling stability of the parallel mode ripples $S_X(\theta)$, extracted from a fit of the x component of Eq. (4) to the data published in our previous work,[12] along with the curvature

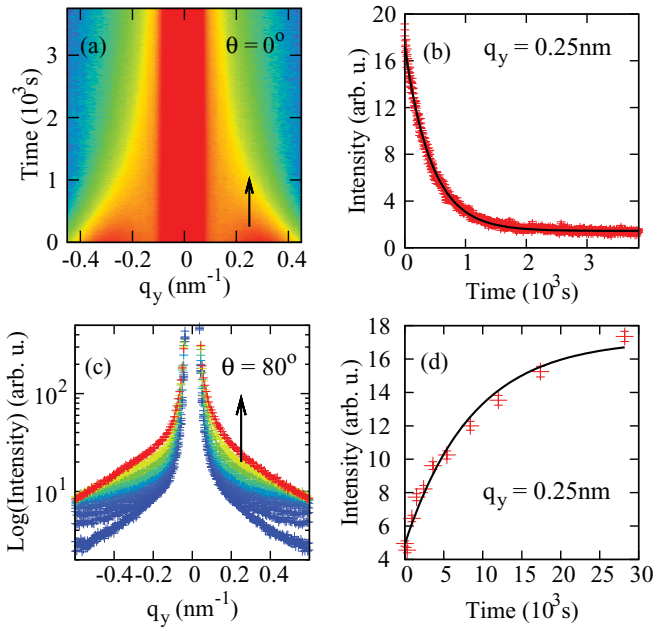

FIG. 1. (Color online) GISAXS *in-situ* measurements of intensity evolution in the q_y direction during normal (0°) and 80° incidence bombardment, respectively. (a) Two-dimensional color logarithmic intensity map of intensity evolution real-time bombardment at normal incidence using an initially rippled surface where blue/medium gray corresponds to low- and red/dark gray to high-scattering intensity. (b) Corresponding plot of the intensity evolution at $q_y =$ 0.25 nm^{-1}, including exponential fit. (c) Scattering *in-situ* time-slice measurements during 80° off-normal bombardment in the q_y direction using an initially smooth surface. Times shown are from $t = 0$ s to $t = 2.8 \times 10^4$ s, where blue/medium gray corresponds to earlier times and red/dark gray to later times. (d) Corresponding intensity plot of one mode $q_y = 0.25$ nm^{-1} including exponential fit. Although the scattered intensity increases, the trend shows exponential relaxation to a new value of dynamic equilibrium.

coefficient controlling the stability of the perpendicular mode ripples $S_Y(\theta)$, extracted from a fit of the y component of Eq. (4) to the data in Fig. 2.

The key factor determining whether a flat surface is stable or unstable at a given bombardment-incidence angle is the sign of the curvature coefficients $S_{X,Y}(\theta)$: they must both be positive for stability. The curvature coefficients $S_{X,Y}(\theta)$ can be broken down further into two components: the BH erosive and Carter-Vishnyakov (CV) redistributive components.[12,17] The erosive contributions $S_{X,Y}^{\text{eros.}}(\theta)$ are evaluated using the modified BH model

$$S_{X,Y}^{\text{eros.}}(\theta) = Ja\Omega\Gamma_{x,y}(\theta)Y(\theta), \quad (5)$$

where $J = 2 \times 10^{12}$ ions/(cm^2 s) is the ion flux, Ω is the Si atomic volume, a is the ion range, $Y(\theta)$ is the incidence angle-dependent sputter yield of a flat surface, and $\Gamma_{x,y}$ represent the curvature coefficients of the yield. All the physical coefficients in $S_{X,Y}^{\text{eros.}}(\theta)$ can be obtained either experimentally or using Monte Carlo simulation of atomic collisions under the Binary Collision Approximation (BCA), e.g., SRIM.[18] Whereas BH used the yield and its curvature dependence from Sigmund's Gaussian ellipsoid model of the collision cascade, we modify

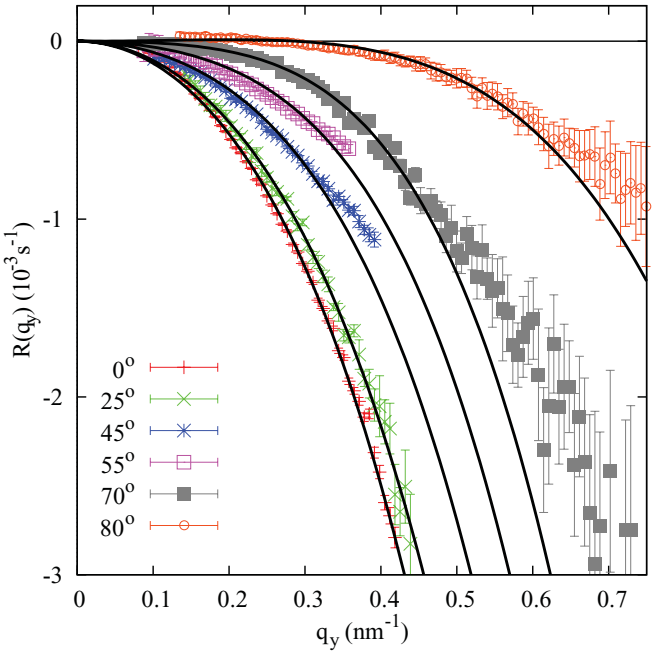

FIG. 2. (Color online) Measured dispersion relations $R(q_y)$ for a wide range of ion-incidence angles θ, including fits using Eq. (4).

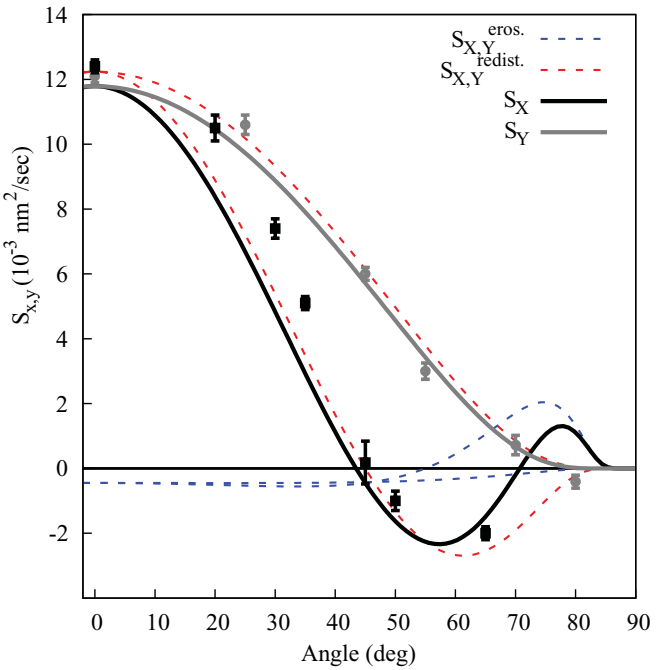

FIG. 3. (Color online) Best fit for the curvature coefficient terms including both x, y orientations including the entire x-direction data set obtained from our previous work. The contribution of the BH erosive component is blue/medium gray and has no free parameter, while the CV redistributive component in red/dark gray has one free parameter. The S term, the sum of the two independent contributions, is shown in black for the x-direction and in gray for the y-direction along with the respective experimental data.

this with the empirical Yamamura correction factor,[19] which was developed to fit the sputter yield vs incidence angle for a large variety of projectiles and targets and was rationalized as accounting for the increasingly incomplete development of the collision cascade as grazing incidence is approached, due to the absence of the solid above the surface. The angular-dependent sputter yield $Y(\theta)$ is reported by Yamamura *et al.* for 1 keV argon ion bombardment of silicon.[19]

We evaluate the ion-stimulated mass redistributive contributions $S^{\text{redist.}}_{X,Y}(\theta)$, using a modified CV/Davidovitch-Aziz-Brenner model for impact-induced mass redistribution,[9,10]:

$$S^{\text{redist.}}_{X}(\theta) = J\delta\Omega\cos(2\theta)\exp\left[\frac{-\Sigma}{\cos(\theta)}\right] \tag{6}$$

$$S^{\text{redist.}}_{Y}(\theta) = J\delta\Omega\cos^2(\theta)\exp\left[\frac{-\Sigma}{\cos(\theta)}\right], \tag{7}$$

where δ is the magnitude of the vector sum of the displacements of all atoms in the collision cascade coming to rest within or on the solid, per incident ion, and the exponential term is the empirical Yamamura correction factor with $\Sigma = 0.827$.[12,19]

The one unknown parameter in $S^{\text{redist.}}_{X,Y}(\theta)$, and therefore $S_{X,Y}(\theta)$, is δ. This is treated as an adjustable parameter to simultaneously optimize the fit of $S^{\text{eros.}}_{X}(\theta) + S^{\text{redist.}}_{X}(\theta)$ to the measured $S_X(\theta)$[12] and $S^{\text{eros.}}_{Y}(\theta) + S^{\text{redist.}}_{Y}(\theta)$ to the measured $S_Y(\theta)$. We obtain a best fit value of $\delta = 70 \pm 5$ nm. The numerical value of δ for 1000 eV impacts is reasonable when compared to recent molecular dynamic simulations yielding $\delta \approx 10$ nm for 250 eV impacts.[17]

The simultaneously optimized fit for $S_X(\theta)$ and $S_Y(\theta)$ and its erosive and redistributive components are superimposed on the data in Fig. 3. It should be noted that although the fitting of $R(q)$ yielded a slightly negative curvature coefficient $S_Y(\theta)$ for the 80° sample, the scattering data there is ambiguous—the experimental amplification factor at low wave numbers is nearly zero. We find that the contribution of the BH erosive components $\mathbf{(}S^{\text{eros.}}_{X}(\theta), S^{\text{eros.}}_{Y}(\theta)\mathbf{)}$, represented by the blue-dashed curves, are negligible within fitting errors except possibly at the most grazing angles of incidence where both erosion and redistribution effects converge to zero; the erosive components are also of the wrong sign to describe the behavior of both $S_X(\theta)$ and $S_Y(\theta)$ over most of the range of θ. The ion-stimulated mass redistribution effect $S^{\text{redist.}}_{X,Y}(\theta)$, represented by the red-dashed curves in Fig. 3, dominates the erosive contribution $S^{\text{eros.}}_{X,Y}(\theta)$ and is essentially the only considerable mechanism for determining smoothening and patterning under uniform ion-beam irradiation except perhaps at the highest ion-incidence angles. These results confirm the conjecture[10,20] that the stability and instability of irradiated surfaces are dominated by impact-induced mass redistribution while erosion plays an insignificant role except possibly at the highest ion-incidence angles where other factors including electrostatic repulsion between the surface potential and the ions as well as shadowing may play important roles as well.

One important "loose end" is to determine the value of the parameter δ independently, from theory or experiment. It can be evaluated directly in molecular dynamics (MD) simulations[1,17] at sufficiently low kinetic energy, but the practicality of direct computation by MD becomes limited with increasing energy. Codes for Monte Carlo simulation of atomic collisions under the BCA are wide spread, e.g., SRIM[18] and SDTrimSP,[21] but their range of validity for this

TABLE I. Magnitude of vector sum of atomic displacements evaluated by three methods for normal-incidence Ar^+ impacts on silicon at two energies. BCA-MC results were obtained from the code SDTrimSP. MD results[17] were obtained using the Environment Dependent Interatomic Potential (EDIP).[22]

δ (nm.atom/ion) For $Ar^+ \rightarrow$ Si impacts at normal incidence			
Energy (eV)	BCA-MC	MD	Fit (this work)
250	3	10	?
1000	9	?	70

purpose needs to be investigated, particularly if the energy is low enough that a significant amount of transport occurs along the surface. In Table I we report values of δ obtained by MD, BCA-MC, and by fitting the experimental dispersion relation to the CV model modified by the empirical Yamamura yield correction, as we have done in this work. We see that the results agree with each other within an order of magnitude, but barely so. Resolving the remaining discrepancies should be a high priority for attaining the goal of parameter-free prediction of pattern formation.

It is conceivable that an erosive mechanism may be significant but that the BH model, which uses the Gaussian ellipsoid approximation for the collision cascades, may simply be a vast underestimate of the erosive contribution to $S_{X,Y}(\theta)$. MD simulations indicate that this is not the case for 250 eV Ar^+ impacts on Si: Norris *et al.*[17,23] have isolated erosive contributions from redistributive contributions by recording the final positions of all displaced atoms and have shown that erosive contributions are indeed negligible. The modified CV model does not fit the redistributive contribution well at this energy, but Norris *et al.* showed that a theoretical upscaling of the MD crater function, which incorporates both erosive and redistributive components but is dominated by the redistributive component, describes the experimental results[24] well with no adjustable parameters.

IV. CONCLUSION

In summary *in-situ* GISAXS enables us to directly measure the dispersion relation $R(\mathbf{q})$ and its dependence on ion-incidence angle, directly giving insight into the physical processes dominating the morphological evolution of the ion-irradiated Si surface. At all angles of incidence the dispersion relation fits well the quadratic-plus-quartic dependence on wave number that is predicted by several models. The dependence on incidence angle of the quadratic coefficient in both the x and y directions is fit well by the CV model of mass redistribution, modified by the empirical Yamamura high-angle correction to the yield. This model has a single adjustable parameter, the magnitude of the vector sum of the atomic displacements per incident ion. We obtain its value by fitting the $S_{X,Y}(\theta)$ data to the sum of this model and the BH erosive term, which has no adjustable parameters but has the empirical Yamamura high-angle correction. The erosive term is nearly two orders of magnitude too small, and of the wrong sign, to explain the results. It is essentially irrelevant, except possibly at the most grazing incidence angles where erosive and redistributive contributions converge to zero. Thus we conclude that the ion-induced lateral mass redistribution contribution is the only significant contribution to the stability and instability of ion-irradiated surfaces for 1 keV Ar^+ bombardment of Si. This is the only system to date for which a physical experiment has yielded a quantitative comparison of erosive and redistributive effects, and the conclusion is corroborated by a MD experiment in the same system at a lower energy.[17]

ACKNOWLEDGMENTS

We thank Peter Siddons and Anthony Kuczewski of Brookhaven National Laboratory for their construction and support of the x-ray detector used in these experiments. We also thank Christie Nelson and Steven LaMarra of the National Synchrotron Light Source for their support and help with beamline X21. E.A. and K.F.L. were supported by NSF DMR-1006538, and C.S.M and M.J.A were supported by DE-FG02-06ER46335. Use of the National Synchrotron Light Source, Brookhaven National Laboratory, was supported by the U.S. Department of Energy, Office of Science, Office of Basic Energy Sciences, under Contract No. DE-AC02-98CH10886.

*eanzenberg@gmail.com

[1]M. Moseler, P. Gumbsch, C. Casiraghi, A. Ferrari, and J. Robertson, Science **309**, 1545 (2005).

[2]C. S. Madi, B. Davidovitch, H. B. George, S. A. Norris, M. P. Brenner, and M. J. Aziz, Phys. Rev. Lett. **101**, 246102 (2008).

[3]W. L. Chan and E. Chason, J. Appl. Phys. **101**, 121301 (2007); G. Ozaydin, A. S. Ozcan, Y. Y. Wang, K. F. Ludwig, H. Zhou, R. L. Headrick, and D. P. Siddons, Appl. Phys. Lett. **87**, 163104 (2005); G. Ozaydin, K. F. Ludwig, H. Zhou, and R. L. Headrick, J. Vac. Sci. Technol. B **26**, 551 (2008); J. Zhou and M. Lu, Phys. Rev. B **82**, 125404 (2010); C. S. Madi, H. B. George, and M. J. Aziz, J. Phys. Condens. Matter **21**, 224010 (2009); R. L. Headrick and H. Zhou, *ibid.* **21**, 224005 (2009); D. Carbone, A. Biermanns, B. Ziberi, F. Frost, O. Plantevin, U. Pietsch, and T. H. Metzger, *ibid.* **21**, 224007 (2009); J. A. Sanchez-Garcia, R. Gago, R. Caillard, A. Redondo-Cubero, J. A. Martin-Gago, F. J. Palomares, M. Fernandez, and L. Vazquez, *ibid.* **21**, 224009 (2009); B. Ziberi, F. Frost, T. Hoche, and B. Rauschenbach, Phys. Rev. B **72**, 235310 (2005); B. Ziberi, M. Cornejo, F. Frost, and B. Rauschenbach, J. Phys. Condens. Matter **21**, 224003 (2009).

[4]G. Ozaydin, K. F. Ludwig, H. Zhou, L. Zhou, and R. L. Headrick, J. Appl. Phys. **103**, 033512 (2008).

[5]B. Ziberi, Ph.D., University of Leipzig, 2006.

[6]Q. Wei, J. Lian, S. Zhu, W. Li, K. Sun, and L. Wang, Chem. Phys. Lett. **452**, 124 (2008).

[7]R. M. Bradley and J. M. Harper, J. Vac. Sci. Technol. A **6**, 2390 (1988).

[8]P. Sigmund, J. Mater. Sci. **8**, 1545 (1973).

[9]G. Carter and V. Vishnyakov, Phys. Rev. B **54**, 17647 (1996).
[10]B. Davidovitch, M. J. Aziz, and M. P. Brenner, Phys. Rev. B **76**, 205420 (2007).
[11]H. Zhou, L. Zhou, G. Ozaydin, K. F. Ludwig, and R. L. Headrick, Phys. Rev. B **78**, 165404 (2008).
[12]C. S. Madi, E. Anzenberg, K. F. Ludwig, and M. J. Aziz, Phys. Rev. Lett. **106**, 066101 (2011).
[13]C. C. Umbach, R. L. Headrick, and K. C. Chang, Phys. Rev. Lett. **87**, 246104 (2001).
[14]S. E. Orchard, Appl. Sci. Res. **11**, A451 (1961).
[15]G. Ozaydin, K. F. Ludwig, H. Zhou, and R. L. Headrick, J. Vac. Sci. Technol. B **26**, 551 (2008); G. Ozaydin-Ince and K. F. Ludwig, J. Phys. Condens. Matter **21**, 224008 (2009).
[16]S. K. Sinha, E. B. Sirota, S. Garoff, and H. B. Stanley, Phys. Rev. B **38**, 2297 (1988).
[17]S. A. Norris, J. Samela, L. Bukonte, M. Backman, F. Djurabekova, K. Nordlund, C. S. Madi, M. P. Brenner, and M. J. Aziz, Nature Commun. **2**, 276 (2011).
[18]J. F. Ziegler, J. P. Biersack, and U. Littmark, *The Stopping and Range of Ions in Matter* (Pergamon Press, New York, 1985).
[19]Y. Yamamura, Y. Itikawa, and N. Itoh, *Angular Dependence of Sputtering Yields of Monatomic Solids* (Institute of Plasma Physics, Nagoya University, Chikusa-ku, Nagoya, Japan, 1983).
[20]M. J. Aziz, Mat. Fys. Medd. Dan. Vid. Selsk. **52**, 187 (2006); N. Kalyanasundaram, M. Ghazisaeidi, J. B. Freund, and H. T. Johnson, Appl. Phys. Lett. **92**, 131909 (2008).
[21]W. Eckstein, R. Dohmen, A. Mutzke, and R. Schneider, *SDTrimSP: A Monte-Carlo Code for Calculating Collision Phenomena in Randomized Targets* (Max-Planck-Institut für Plasmaphysik, Greifswald, Germany, 2007).
[22]M. Z. Bazant, E. Kaxiras, and J. F. Justo, Phys. Rev. B **56**, 8542 (1997).
[23]S. A. Norris, M. P. Brenner, and M. J. Aziz, J. Phys. Cond. Matt. **21**, 224017 (2009).
[24]C. S. Madi, H. B. George, and M. J. Aziz, J. Phys. Condens. Matter **21**, 224010 (2009).